et al.[2,3] and Costello *et al.*[6,7] Since it is known that water vapor and the heavier hydrocarbons are present in vacuum systems,[25] further experimental work with these gases is needed.

Results show that variations in target thickness remains as a problem and that improvement in target preparation methods is needed.

Work is now in progress toward improvement of the resolution of the electrostatic analyzer used for this work. With better resolution, further progress is expected toward reducing the uncertainties remaining in regard to the factors which determine the form of resonance yield curves.

Reproducibility of energy standards and intercomparison of these standards between laboratories will then be more straightforward and determination of nuclear resonance widths from yield curve shapes may be more commonly realized.

ACKNOWLEDGMENTS

The authors are indebted to Professor M. B. Webb, C. H. Blanchard, K. R. Symon, and H. W. Lewis for many helpful discussions. In particular the authors are indebted to Professor E. Merzbacher for his help with the collision spectrum. The expert aid of M. F. Murray in his design of the electronics used in this work is appreciated. The authors also wish to thank R. J. Nickles, K. E. Nielsen, and R. A. Due who assisted in taking the data.

PHYSICAL REVIEW VOLUME 135, NUMBER 5A 31 AUGUST 1964

Proton Energy-Loss Distributions from Thin Carbon Films*

A. L. MORSELL†
University of Wisconsin, Madison, Wisconsin
(Received 17 January 1964; revised manuscript received 1 May 1964)

A 992-keV proton beam, limited in energy spread by a 1-m electrostatic analyzer, passes through a thin carbon film before entering a second 1-m electrostatic analyzer. The energy distribution of protons in the second analyzer is measured by sorting proton counts from a detector at the analyzer exit according to the instantaneous value of a sweep voltage applied to one of the analyzer plates. A combined resolution of 30 000 was obtained for the double-analyzer system. Carbon films with thicknesses corresponding to mean energy losses ranging from several keV down to about 200 eV have been studied. Several of the experimental energy-loss distributions are compared with distributions computed by Monte Carlo techniques for three different assumed discrete energy-loss spectra. Good fits are obtained from a new spectrum constructed using the results of some computations by E. Merzbacher.

INTRODUCTION

THE statistical process by which high-energy charged particles lose energy as they interact with the atomic electrons of a target material may be completely described by what will be called the discrete energy-loss spectrum, a function which gives the probabilities for energy-loss jumps of varying magnitudes. This function is needed for proper handling of the energy-loss process in many experimental situations; knowledge of the stopping power of the target material or of the range of the high-energy particles in the material is often not sufficient. Unfortunately, the discrete energy-loss spectra are not available in the literature in any convenient form, and there has been virtually no experimental effort directed toward determining them.

The present work represents an attempt to obtain measurements which will provide information about these fundamental functions. A nearly monoenergetic beam of protons is allowed to pass through a thin carbon film, and the resultant energy-loss distribution of the protons is measured. If the target film is thin enough and the resolution high enough, the energy-loss distribution should be a moderately sensitive function of the discrete energy-loss spectrum of the material. An attempt is made to construct a close approximation to the true discrete energy-loss spectrum for use in computing energy-loss distributions to be compared with the experimental results.

DESCRIPTION OF THE EXPERIMENT

The physical layout of the experiment is schematically shown in Fig. 1. The proton beam from the 3-MeV Wisconsin Electrostatic Accelerator, after passing through a magnetic analyzer and a pair of electrostatic quadrupole lenses, traverses a cylindrical electrostatic analyzer, which selects only those protons with energies close to a mean energy determined by the potentials on the cylindrical plates. The protons then pass through a target film and traverse a second electrostatic analyzer. Protons selected by this analyzer are scattered by

* Work supported in part by the U. S. Atomic Energy Commission.
† Present address: High Voltage Engineering Corporation, Burlington, Massachusetts.

several layers of gold leaf. Those protons intercepted by a solid-state detector behind the gold leaf are registered as counts in a multichannel analyzer. The detector is mounted on an arm which pivots about an axis passing vertically through the gold leaf scatterer. Because of the $1/\sin^4(\frac{1}{2}\theta)$ dependence of the Rutherford scattering cross section, the proton counting rate drops rapidly as the detector is swung away from the beam axis. Thus, the counting rate, controlled by positioning the detector, may be maintained at a level easily handled by the electronics. The relationships among the various electronic components are shown in Fig. 2. Although the analyzer voltage supply is very well regulated, the remaining voltage fluctuations require compensating circuitry. Since the double analyzer system measures the difference in energy between protons selected by the first analyzer and protons selected by the second analyzer, the measurement will be undisturbed by voltage fluctuations if these fluctuations cause identical selection energy fluctuations in each analyzer. This condition is fairly well approximated by the circuit shown in the figure. The inside plate of the second analyzer is directly connected to the inside plate of the first. Because the plate spacings of the analyzers are such that the second analyzer requires less voltage than the first, the first analyzer outside plate potential is attenuated to provide the potential for the second analyzer outside plate. Attenuation is achieved through the voltage divider and cathode follower shown in the figure.

The second electrostatic analyzer is caused to sweep over a convenient range of proton energies by a time-varying sweep voltage superposed on the steady potential of the outside analyzer plate. The sweep signal, which has a very linear sawtooth waveform, is applied to the low-voltage side of the voltage divider. The same signal is applied to the pulsemaker, which converts discriminator pulses that have been triggered by the amplified detector pulses into new pulses with amplitudes proportional to the instantaneous value of the sweep voltage. A Nuclear Data 256-channel pulse-height analyzer counts the new pulses while sorting them according to their amplitudes. There is a linear relationship between the energy of protons registered as counts in a particular counting channel and the number of that channel. After counting for many sweep cycles, the multichannel analyzer readout gives an accurate representation of the energy-loss distribution of protons entering the second analyzer. This energy-loss distribution takes the form of a list of counts per channel for about 80 channels. Since it is easy to vary the steady potential to which the sweep is added, the energy range can be extended by taking several data groups with overlapping end points, each group representing only a portion of the distribution function. The overlapping points are used when fitting the portions of the distribution together to form a single continuous curve.

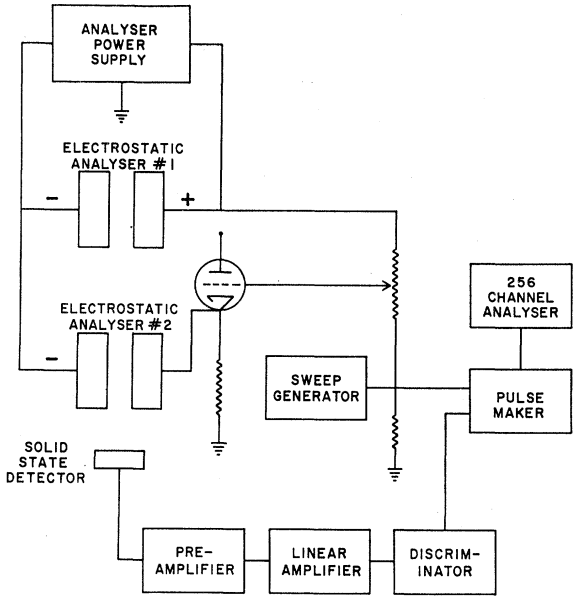

FIG. 2. Block diagram of the instrumentation.

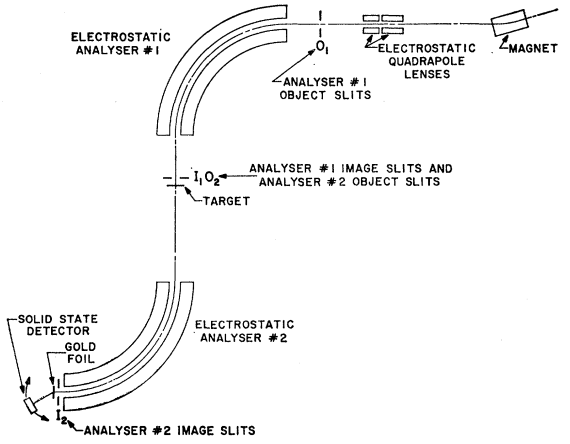

FIG. 1. Physical layout. The widths of slits O_1 and I_1O_2 are both about 0.01 mm and the width of slit I_2 is about 0.005 mm.

RESOLUTION OF THE DOUBLE ANALYZER SYSTEM

When the target is removed from the beam path and the second analyzer is used to examine the beam from the first analyzer, the observed beam energy distribution has the form of a plot of proton counts versus channel number, where the channel number is linearly related to the proton selection energy of the second analyzer. It is not obvious what conditions must be satisfied in order that the observed energy distribution be an accurate replica of the actual beam energy distribution at the target position. A careful analysis[1] of

[1] A. L. Morsell, Ph.D. thesis, University of Wisconsin, 1963 (unpublished); available from Ann Arbor Microfilms, Ann Arbor, Michigan.

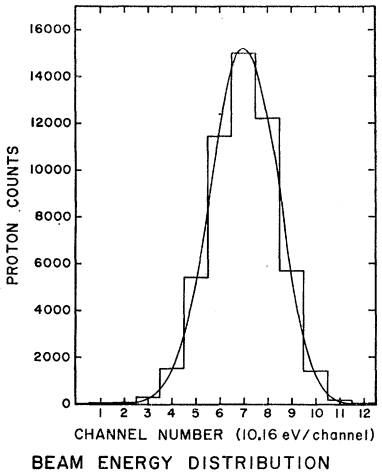

FIG. 3. Observed beam energy distribution for 992-keV protons. (The direction of increasing energy is toward the right.)

this problem, performed some time after the experimental data had been taken, revealed that the asymmetric S-shaped configuration for the two analyzers was not the best possible choice. For the chosen configuration and under otherwise ideal conditions the width at half-maximum of the observed beam energy distribution is a factor of 1.78 greater than the width of the true energy distribution of the beam from the first analyzer, and the shape of the true distribution is badly misrepresented. The ideal configuration is a symmetric, C-shaped arrangement. Then, for a proper choice of slit-widths, the observed beam-energy distribution is identical to the true distribution.

The combined resolution for the two analyzers is defined as the ratio of the mean beam energy to the width at half-maximum of the observed beam-energy distribution. The combined resolution computed from the dimensions and parameters of the analyzers is 50 000. The best combined resolution actually obtained from the double-analyzer system was 30 000. To get this value it was necessary to limit the vertical extent of the proton beam to about 0.06 mm by installing apertures at the entrance and exit of the first analyzer. The need for these very narrow apertures was explained after the experiment was dismantled. It was found that the plates of the first analyzer were warped and that magnetic fields with radial components of about 20 G existed between the plates.

Figure 3 shows the observed beam-energy distribution for the conditions under which most of the experimental energy-loss distributions were obtained. The histogram is a plot of the 256-channel analyzer output for a counting run 30 min long, and the smooth curve is an attempt to guess at the true shape of the distribution. The mean proton energy was 992 keV, and the width at half-maximum of this distribution is about 33 eV.

PREPARATION OF THE CARBON FILMS

Carbon is evaporated in an evacuated bell jar onto freshly split mica sheets. The evaporated films are removed from the mica by slowly lowering the mica sheets into distilled water, and the films are picked up from the surface of the water on holders with one or more small holes. Both thin tantalum sheets with punched 1-mm-diam round holes and flat nickel screen with $\frac{1}{2}$-mm square holes have been successfully used as film holders.

After the films are mounted in the target chamber at the exit of the first analyzer, they are decreased in thickness by a technique developed at Wisconsin by T. Pauly and R. G. Herb.[2] The films are bombarded by atomic hydrogen from a source consisting of a hot (about 2400°K) tungsten filament in a 1.25-cm i.d. Pyrex tube; some of the hydrogen bled into the tube is converted to atomic form by the hot filament and escapes *via* a small hole in the side of the tube about $\frac{1}{2}$ cm from the carbon film. The atomic hydrogen, reacting with the carbon to form methane, very rapidly reduces the thickness of the film. During the thinning process the hydrogen pressure in the target chamber is about 5×10^{-4} Torr. Thinning times of less than one minute are sufficient to produce noticeable changes in the measured energy-loss distributions.

COMPUTATIONAL PROCEDURE

The straggling theory in the literature does not apply to the results of this experiment, since the approximations used in the theory are not valid for very thin absorbers. In order to demonstrate the effect of different assumptions for the discrete energy-loss spectrum, a more exact computational procedure was developed and is presented in this section.

Let E_0 be the mean energy of the beam incident

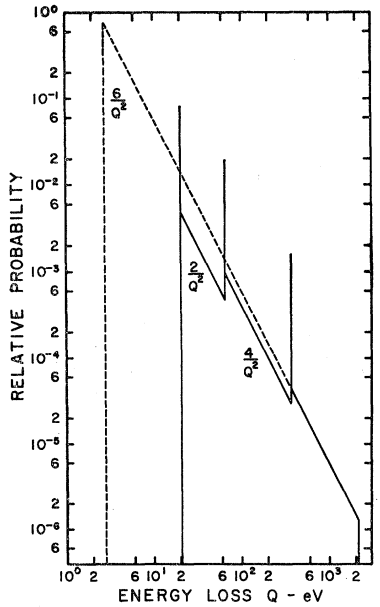

FIG. 4. Log-log plot of the simple free-electron spectrum (dashed line) and the Costello-Skofronick spectrum (solid line) for 992-keV protons interacting with carbon.

[2] T. Pauly and R. G. Herb (private communications).

on the target, let E_f be the energy of a particular proton after it has passed through the target, and let $E_0-E_f=\mathcal{E}$. Then there exists a function $P(\mathcal{E},x)$ such that $P(\mathcal{E},x)d\mathcal{E}$ gives the probability that a proton has energy E_f somewhere in the interval $(E_0-\mathcal{E}, E_0-\mathcal{E}-d\mathcal{E})$ after having passed through a target of thickness x. The expression $P(\mathcal{E},0)=D(\mathcal{E})$ represents the initial beam-energy distribution. Because the target thickness x in distance units is not known for the carbon films, mean energy loss $\mathcal{E}'=\int_{-\infty}^{\infty}\mathcal{E}P(\mathcal{E},x)d\mathcal{E}$, where P is the experimentally observed energy-loss distribution, is used to characterize the target thickness.

The discrete energy-loss spectrum $\chi(Q)$ is defined such that $\chi(Q)dQdx$ is the probability that a proton, while traveling distance dx in the target, will suffer a collision in which the proton loses an energy between Q and $Q+dQ$. The function χ depends on the proton energy E as well as on the discrete energy loss Q. However, the range of E for very thin target films is small compared to E_0, and it is a good approximation to treat χ as a function only of Q. The mean energy loss per collision is $Q'=\int_0^{\infty}Q\chi(Q)dQ/\int_0^{\infty}\chi(Q)dQ$. It can be shown that the average number of collisions M suffered by protons in a target of thickness $\mathcal{E}'$ is $M=\mathcal{E}'/Q'$.

The distributions $P(\mathcal{E},x)$ for particular fixed values of x have been computed from certain contrived functions $\chi(Q)$ using Monte Carlo techniques. The computed distributions are then compared with the experimental distributions in the hope of determining the actual form of χ. The Monte Carlo calculations are carried out using

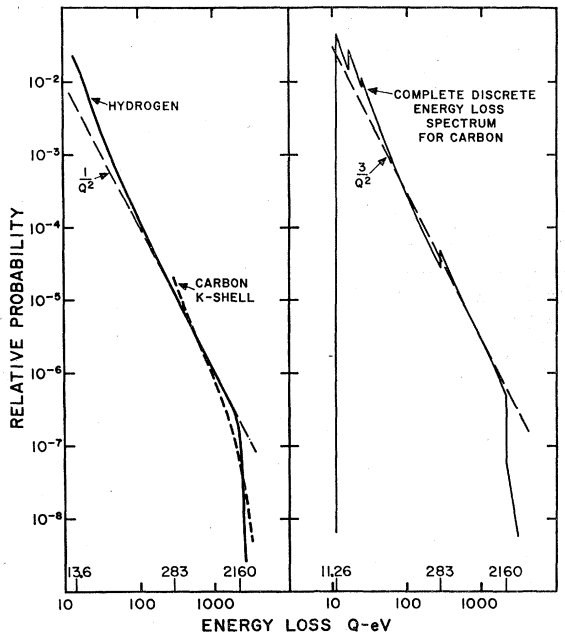

FIG. 5. The left-hand side is a log-log plot of the discrete energy-loss spectra computed by Merzbacher for hydrogen, and for the K-shell electrons of carbon. The right-hand side shows the new spectrum for 992-keV protons interacting with carbon.

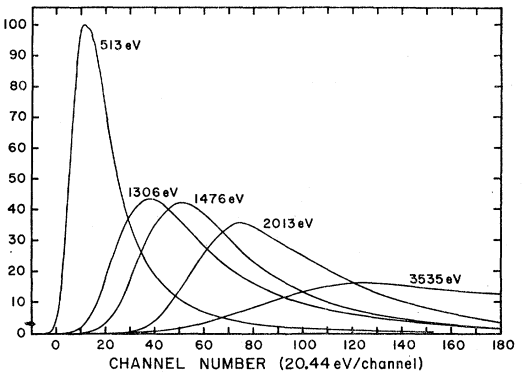

FIG. 6. Energy-loss distributions from films prepared without using the thinning process.

a method suggested in a paper by J. R. Herring and E. Merzbacher.[3] A total number of protons N is divided up into groups N_k according to the Poisson distribution $W(k)=M^k e^{-M}/k!$ in such a way that $N_k/N=W(k)$. Here $M=\mathcal{E}'/Q$, where Q' is computed from the hypothesized discrete energy-loss spectrum $\chi(Q)$, and N_k is the number of protons which suffer just k collisions while traversing a target of thickness $\mathcal{E}'$. A total energy loss ϵ for one of these N_k protons is determined by generating k discrete energy losses Q_i and summing them, so that $\epsilon=\sum_{i=1}^{k}Q_i$. This process is repeated for each of the protons in each of the collision number groups. The N values of ϵ are sorted and tabulated to generate a distribution $P_0(\epsilon)$, which represents a proton energy-loss distribution for an initially monoenergetic beam. The experimentally observed beam energy distribution $D(\mathcal{E})$ of Fig. 3 is numerically folded into $P_0(\epsilon)$ according to the equation $P(\mathcal{E})=\int D(\mathcal{E}-\epsilon)P_0(\epsilon)d\epsilon$ to obtain the final distribution $P(\mathcal{E})$, which is to be compared with the experimental data.

The discrete energy losses Q_i are generated by first storing an indexed list of 16 384 different Q values in the memory of the computer and then generating random indices R from 1 to 16 384 to select various Q's from the list. The Q values in the list are determined by a function $Q(R)$, which is obtained by inverting the relationship

$$R(Q)=R_{\max}\int_{Q\min}^{Q}\chi(Q')dQ'\Big/\int_{Q\min}^{Q\max}\chi(Q')dQ'. \quad (1)$$

This relationship is a result of the requirement that the Q's in the list be distributed according to the spectrum $\chi(Q)$.

SEVERAL DISCRETE ENERGY-LOSS SPECTRA FOR USE IN THE COMPUTATIONS

The classical theory for the interaction of protons with stationary free electrons gives the following ex-

[3] J. R. Herring and E. Merzbacher, J. Elisha Mitchell Scientific Soc. 73, No. 2 (1957).

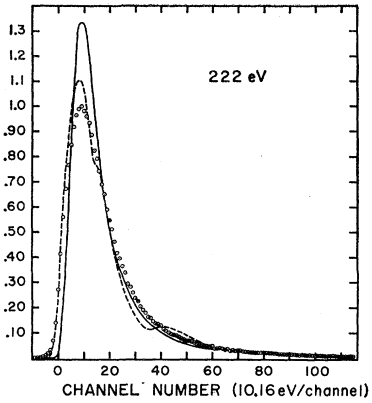

FIG. 7. Comparison between the 222-eV experimental distribution and distributions computed from the simple spectrum (the solid line) and the C-S spectrum (the dashed line).

pression[4] for the discrete energy-loss spectrum:

$$\chi(Q)dQ=(2\pi e^4/mV^2)NZ(dQ/Q^2)\,, \qquad (2)$$

where e is the electronic charge, m is the mass of the electron, V is the proton velocity, N is the number of target atoms per cm^3, and Z is the atomic number of the target material. The laws of conservation of energy and momentum place an upper bound $Q_{\max}$ on the amount of energy which may be lost by a proton in a single collision with an electron. It can be shown that $Q_{\max}\doteq 2mV^2$, which equals 2160 eV for a proton energy of 992 keV. A lower bound $Q_{\min}$ is determined by the requirement that the stopping power

$$d\mathcal{E}/dx=\int_{Q\min}^{Q\max} Q\chi(Q)dQ \qquad (3)$$

be equal to the stopping power given by the well-known formula of H. Bethe,[5] which may be written for the case of nonrelativistic protons as

$$\frac{d\mathcal{E}'}{dx}=\frac{4\pi e^4}{mV^2}NZ\ln\left(\frac{2mV^2}{I}\right). \qquad (4)$$

The quantity I is called the geometric mean excitation potential. Its value for carbon is about 78 eV.[6] Then $Q_{\min}$ is found to be 2.82 eV.

Since the atomic electrons of the target material are neither stationary nor free, the actual function $\chi(Q)$ may be expected to deviate considerably from the classical expression. These considerations led Costello and Skofronick[7] to formulate a discrete energy-loss spectrum which takes into account the electron binding. This function is constructed according to the following recipe: Let $\chi(Q)=\sum_n\chi_n(Q)$, and

$$\chi_n=(2\pi e^4/mV^2)NZ_n[1/Q^2+C_n\delta(I_n-Q)] \qquad (5)$$

for $I_n\leqslant Q\leqslant Q_{\max}$, $\chi_n=0$ for $Q<I_n$, and $Q>Q_{\max}$. The index n refers to a group of Z_n electrons with binding energy E_n in a particular atomic shell or subshell. The values of I_n are chosen to satisfy the relationships $I_n\propto E_n$ and $Z\ln(I)=\sum_n Z_n\ln(I_n)$. The constants C_n are chosen so that the stopping power contribution from the δ-function term just equals the contribution from the $1/Q^2$ term for each electron group. It can then be easily shown that the stopping power computed from this contrived function $\chi(Q)$ will exactly match the Bethe formula. From values for E_n for the $2p^2$, $2s^2$, and $1s^2$ electrons of carbon given by Sternheimer,[6] the I_n values are determined to be 20.6, 65, and 365 eV, and the constants C_n are 0.226, 0.0538, and 0.00488 (eV)$^{-1}$. The resulting spectrum is shown in Fig. 4 by the solid lines; the dashed lines in the figure represent the simple free-electron spectrum.

A new spectrum has been constructed using the re-

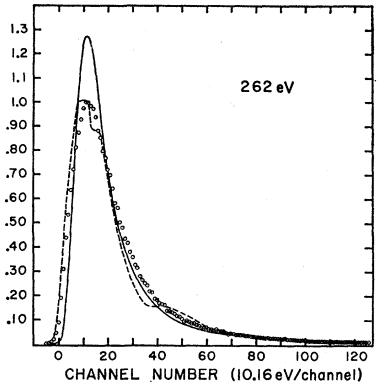

FIG. 9. Comparison between the 262-eV experimental distribution and distributions computed from the simple spectrum (the solid line) and the C-S spectrum (the dashed line).

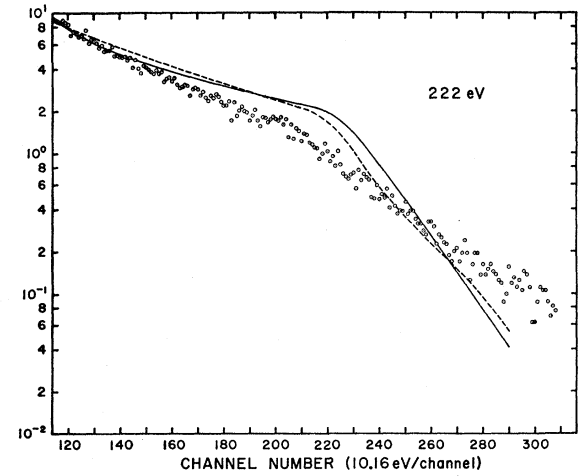

FIG. 8. Semilog plot of the tails of the distributions of Fig. 7.

[4] R. D. Evans, *The Atomic Nucleus*, (McGraw-Hill Book Company, Inc., New York, 1955), Chap. 18.
[5] H. Bethe, Ann. Physik **5**, 325 (1930).
[6] R. M. Sternheimer, Phys. Rev. **88**, 851 (1952).
[7] J. G. Skofronick and D. G. Costello, Bull. Am. Phys. Soc. **8**, 320 (1963); D. G. Costello, J. G. Skofronick, A. L. Morsell, D. W. Palmer, and R. G. Herb, Nucl. Phys. (to be published).

sults of some computations by E. Merzbacher,[8] who has used the Born approximation to obtain discrete energy-loss spectra for the special cases of 1-MeV protons interacting with hydrogen and 992-keV protons interacting with the K-shell electrons of carbon. These functions are shown on the left-hand side of Fig. 5. Both of these functions are assumed to drop to zero for Q values below the binding energy of the electrons; it may be argued that since the discrete atomic energy levels are dense only near the continuum levels, the lower discrete levels will contribute negligibly to the energy-loss process.

The spectra of Merzbacher have been used to construct the complete spectrum for carbon shown on the right-hand side of Fig. 5. This new spectrum is written in the form $\chi=\chi_K+\sum_n\chi_n$. Merzbacher's carbon K-shell spectrum is used for the term χ_K, and the terms χ_n correspond to L-shell electrons with various binding energies. Since the values for these binding energies are of about the same magnitude as the ionization potential

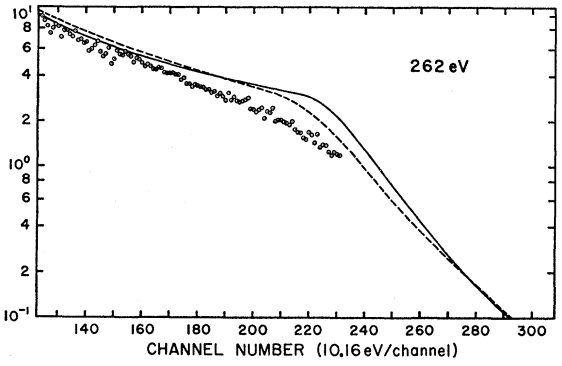

FIG. 10. Semilog plot of the tails of the distributions of Fig. 9.

of hydrogen, it is assumed that each of these terms may be approximated by a function similar in shape to Merzbacher's spectrum for hydrogen. Each term is given the form

$$\chi_n(Q)=(2\pi e^4/mV^2)NZ_n(1/Q^2+C_n/Q^{3.28}) \qquad (6)$$

for $E_n\leqslant Q\leqslant 2160$ eV, $\chi_n(Q)=0$ for $Q<E_n$, and $Q>2160$ eV. This function closely approximates the spectrum for hydrogen when $Z_n=1$, $E_n=13.6$ eV, and $C_n=86.0$.

A binding energy E_n is defined as the energy required to remove a particular electron from an isolated carbon atom without disturbing the other atomic electrons. Values for E_n are obtained from energy level tables[9] compiled by the National Bureau of Standards. The conventional ionization potential, $E_1=11.26$ eV, is the value of E_n for the two $2p$ electrons, and $Z_1=2$. The energy required to remove one of the $2s^2$ electrons is

[8] E. Merzbacher (private communication); computer programming by G. S. Khandelwal.

[9] Natl. Bur. of Stds. (U.S.), Circ. 467, Vol. I (1900).

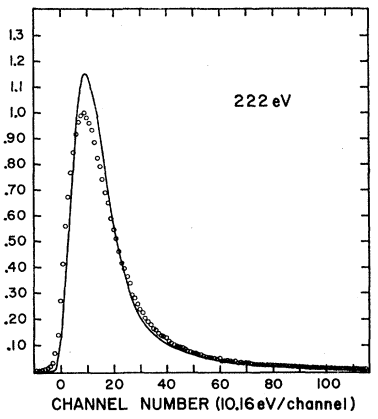

FIG. 11. Comparison between the 222-eV experimental distribution and a distribution computed from the new spectrum.

11.26 eV plus the energy required to excite the carbon ion from the ground state L-shell configuration $2s^22p$ to a level with the configuration $2s2p^2$. There are two such levels corresponding to different final spin directions for the remaining $2s$ electron, allowed by the assumption that removal of a $2s$ electron will not alter the total orbital angular momentum of the atom. Then the binding energies for the $2s$ electrons are found to be $E_2=16.60$ eV and $E_3=24.96$ eV, and the values $Z_2=\frac{4}{3}$ and $Z_3=\frac{2}{3}$ are deduced from the multiplicities of the ionic levels.

The constants C_n are determined in part by the requirement that the stopping power computed from the new spectrum match the stopping power computed from the Bethe formula including a correction given by M. C. Walske[10] for the effect of the large binding energy of the K-shell electrons. This requirement, plus the rather arbitrary assumption that the stopping power contribution from each $C_n/Q^{3.28}$ term should be proportional to the stopping power from the corresponding

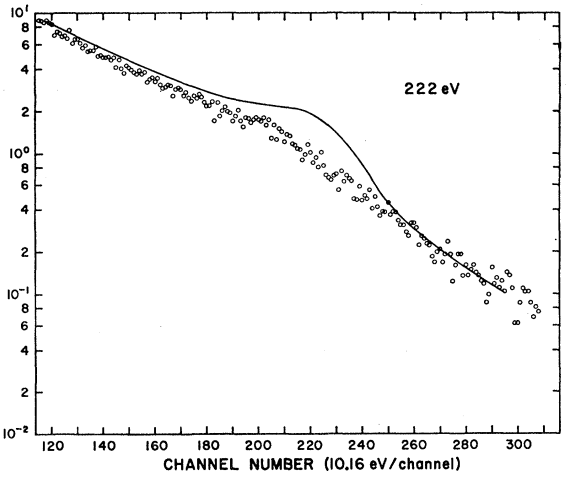

FIG. 12. Semilog plot of the tails of the distributions of Fig. 11.

[10] M. C. Walske, Phys. Rev. 88, 1283 (1952).

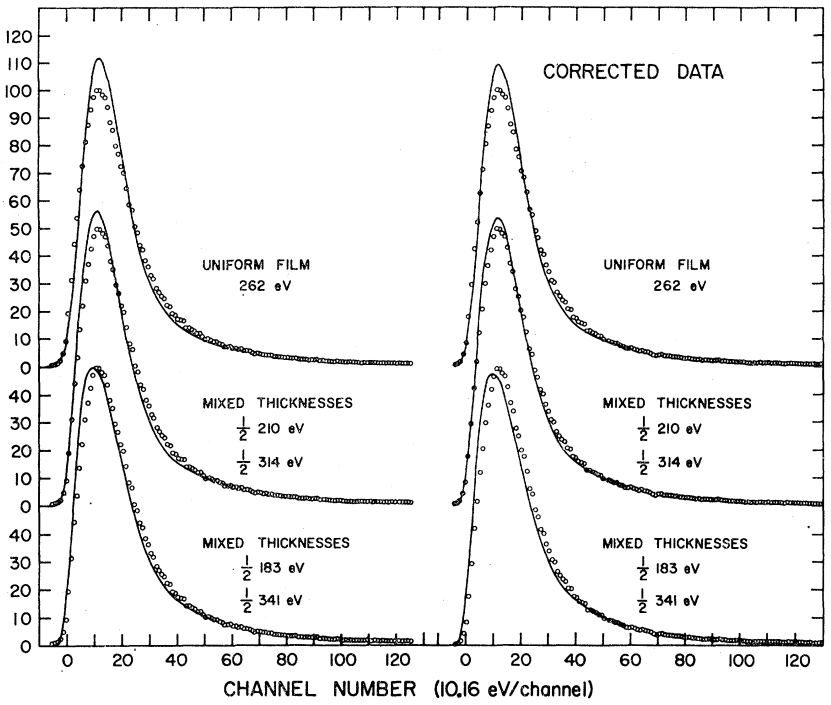

FIG. 13. Comparison between the 262-eV experimental distribution and several distributions computed from the new spectrum for different degrees of target nonuniformity. A correction for dead time in the 256-channel analyzer has been applied to the three identical sets of experimental points on the right-hand side of the figure.

$1/Q^2$ term, result in the values $C_1=105$, $C_2=159$, and $C_3=249$.

COMPARISON OF THE EXPERIMENTAL DATA WITH THE MONTE CARLO DISTRIBUTIONS

Figure 6 shows some energy-loss distributions obtained from carbon films prepared without using the atomic hydrogen thinning process. The data are normalized so that each distribution represents the same total number of proton counts. In this and the remaining figures, the direction of increasing energy is toward the left; the proton energy *loss* is proportional to channel number. The mean energy-loss values given in the figure are computed from the experimental distributions and may be related to the film thickness by the simple expression $\mathcal{E}'=(d\mathcal{E}'/dx)x$, where x is the target thickness, $\mathcal{E}'$ is the mean energy loss, and $d\mathcal{E}'/dx$ is the stopping power, determined from the corrected Bethe formula to be 5.16 eV/Å.

Much thinner targets could be obtained by using the atomic hydrogen thinning technique. The two best energy-loss distributions measured for thinned targets are shown in Figs. 7 through 14, where the experimental distributions are compared with computed curves. The experimental data points are plotted as small circles, while the computed distributions are represented by continuous curves. Each computed curve has the same area beneath it and the same computed $\mathcal{E}'$ as the experimental distribution with which it is plotted. The distribution labeled 262 eV is the most accurate set of experimental data, and the distribution labeled 222 eV represents the only thin film for which the tail of the distribution was measured out to large total energy loss values.

Figure 7 shows a comparison between an experimental distribution with $\mathcal{E}'=222$ eV and two computed curves, one obtained using the simple spectrum (the solid line) and one obtained from the Costello-Skofronick (C-S) spectrum (the dashed line). A separate semilog plot of the tails of the distributions is shown in Fig. 8 to demonstrate the effect of the classical high-energy cutoff at 2160 eV. Figures 9 and 10 show a similar set of distributions for a target with a thickness of 262 eV. An examination of Figs. 7 and 9 reveals that, though the curves computed from the C-S spectrum give a better fit to the experimental data than do the curves from the simple spectrum, the C-S spectrum results in wiggles which were not experimentally observed. In none of the experimental curves are there wiggles which cannot be explained by the statistical deviations of the data points.

Figures 11 and 12 show the 222-eV experimental distribution plotted with a curve computed from the new spectrum. This computed distribution has no discernible wiggles; and though there might be some question about the quality of the fit to the experimental points over the low-energy-loss portion of the distribution, the new spectrum certainly gives a better fit out on the tail. The improved fit beyond the classical cutoff is due to the fact that the new spectrum allows some discrete energy losses (for K electrons) greater than the cutoff value of 2160 eV, whereas the simple and the C-S spectra do not. It is clear that the fit would have been still better if the L-shell portion of the new spec-

trum had not been cut off sharply at 2160 eV, but instead had been given the shape of the high-energy-loss part of the Merzbacher spectrum for hydrogen.

It has been tacitly assumed up to this point that the target films are uniform in thickness. However, during the process of trying to fit the experimental data with computed curves, it became evident that it would be necessary to assume rather large degrees of nonuniformity. In order to simplify the computations, it is assumed that the target is composed of just two different thicknesses, chosen so that the average thickness is equivalent to the value of $\mathcal{E}'$ computed from the experimental distribution. Then the computed distribution is simply the sum of two distributions computed for two different values of $\mathcal{E}'$ and weighted according to the apportionment of target area between the two thicknesses.

Even with this freedom to choose varying degrees and types of nonuniformity, it is difficult to obtain good fits until a correction for dead time in the 256-channel analyzer is applied to the experimental data. For this experiment pulses of different amplitudes are not randomly mixed as they are for the usual sort of pulse-height spectrum measurement; the dead time error is different from that usually encountered; and the effect of applying the dead-time correction is to increase the height of the peak of the experimental distribution relative to the tail of the distribution. Because the beam intensity fluctuated widely during the counting runs, the true amount of dead-time error is unknown and could be several times the minimum value calculated asuming a constant beam intensity.

A dead-time correction twice as great as the minimum correction has been applied to the 262-eV experimental distribution. The uncorrected and the corrected data points are plotted on the left and right sides, respectively, of Fig. 13. The solid lines are distributions computed from the new spectrum; the upper curves represent a film of uniform thickness, the middle curves were calculated assuming a half-and-half mixture of the thickness 210 and 314 eV, and the lower curves were calculated assuming a half-and-half mixture of the thicknesses 183 and 341 eV.

Two types of target nonuniformity quite different from the half-and-half mixture of thicknesses are shown in Fig. 14, where the solid line demonstrates the effect of high bumps covering one-fourth of the target area, and the dashed line demonstrates the effect of deep holes covering one-fourth of the target area. The new spectrum is used for the computed curves, and the 262-eV experimental distribution is not corrected for dead time.

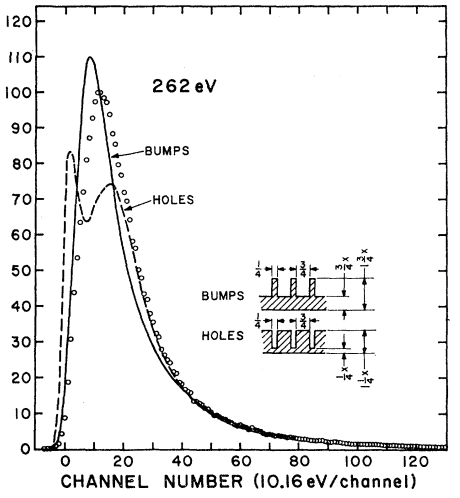

FIG. 14. Comparison between the 262-eV experimental distribution and distributions computed from the new spectrum for two different types of target nonuniformity.

It is evident from these figures that the best fit is obtained when the data is corrected for dead time, and when the 210- and 314-eV half-and-half mixture of thicknesses is assumed. There is no reason to suppose that this combination of discrete energy-loss spectrum target nonuniformity, and dead-time correction is the only combination which will yield a good fit. However, it is gratifying that a fit can be obtained using the new spectrum with what appear to be reasonable assumptions for the other unknowns.

Conclusions are severely limited by the uncertainties in target thickness. A microscopic measurement of target-film uniformity would have been desirable, but was not attempted since such a measurement appeared forbiddingly difficult. The thinned carbon films were extremely fragile and could not be transferred from the evacuated target chamber.

ACKNOWLEDGMENTS

The author would like to express his appreciation to Professor R. G. Herb for his active support and guidance during the course of this work. The author is indebted to Professor E. Merzbacher for many helpful discussions regarding the calculations and for his kindness in furnishing the results of computations performed expressly for the conditions of this experiment. It is a pleasure to acknowledge the expert aid of M. F. Murray in the design of much of the electronic apparatus and to acknowledge the skillful help of R. A. Due, who prepared most of the carbon films and spent many long hours assisting with the taking of data.